JACS
JOURNAL OF THE AMERICAN CHEMICAL SOCIETY
Article
pubs.acs.org/JACS

Probing Polytopic Membrane Protein–Substrate Interactions by Luminescence Resonance Energy Transfer

Monika Musial-Siwek, Marcie B. Jaffee,[§] and Barbara Imperiali*

Departments of Biology and Chemistry, Massachusetts Institute of Technology, Cambridge, Massachusetts 02139, United States

Supporting Information

ABSTRACT: Integral membrane proteins play essential roles in all living systems; however, major technical hurdles challenge analyses of this class of proteins. Biophysical approaches that provide structural information to complement and leverage experimentally determined and computationally predicted structures are urgently needed. Herein we present the application of luminescence resonance energy transfer (LRET) for investigating the interactions of the polytopic membrane-bound oligosaccharyl transferases (OTases) with partner substrates. Monomeric OTases, such as the PglBs from *Campylobacter jejuni* and *Campylobacter lari*, catalyze transfer of glycans from membrane-associated undecaprenol diphosphate-linked substrates to proteins in the bacterial periplasm. LRET-based distance measurements are enabled by the inclusion of an encoded *N*-terminal lanthanide-binding tag (LBT), and LRET between the luminescent (LBT)-Tb^{3+} donor complex and fluorescently labeled peptide and glycan substrates provides discrete distance measurements across the span of the membrane. LRET-based measurements of detergent-solubilized PglB from *C. lari* allowed direct comparison with the distances based on the previously reported the *C. lari* PglB crystal structure, thereby validating the approach in a defined system. Distance measurements between peptide and glycan substrates and the *C. jejuni* PglB offer new experimental information on substrate binding to the related, but structurally uncharacterized, eukaryotic OTase.

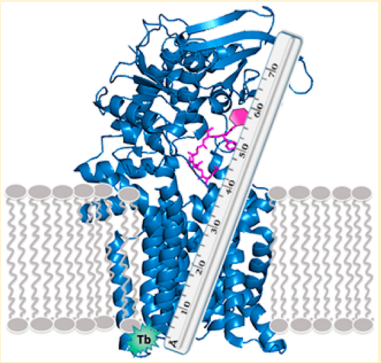

INTRODUCTION

Integral membrane proteins are estimated to comprise approximately 30% of all proteomes,[1] yet they only represent a small fraction of structures deposited in the protein data bank (PDB).[2,3] This important class of proteins plays essential functions in cellular transport, signal recognition and transduction, bioenergetics, and cell–cell communication, making many of the members attractive targets for drug development.[4] However, understanding the structures and interactions of integral membrane proteins is hampered by technical challenges associated with the application of analytical biophysical approaches. In particular, these flexible and unstable proteins are among the most challenging to study because access to quantities of purified proteins from heterologous expression is often hindered by cellular toxicity[5] and protein solubility upon extraction from native membrane environments.[6] As of early 2015, there were 533 unique X-ray structures of membrane proteins deposited in the PDB.[7] Furthermore, progress has also been made in the application of other approaches, including electron cryo-microscopy (cryo-EM),[8] MicroED,[9] and solid state NMR,[10] for deriving the structures of integral membrane proteins. While these challenging and labor-intensive approaches often provide the first glimpses into the structures of target membrane proteins, we sought to establish a general strategy, employing a sensitive spectroscopic ruler based on luminescence resonance energy transfer (LRET) pioneered by Selvin and co-workers[11−13] and enabled by encoded lanthanide-binding tags (LBTs).[14] This approach provides substrate-binding information and affords discrete distance measurements across the span of the membrane. LRET-based techniques have been used to study the functions and dynamics of large protein complexes. In particular, lanthanide-binding sites have been introduced by chemical modification for the study of ion channels[15,16] and encoded Tb^{3+} binding sites have been introduced into lactose permease, a membrane transporter,[17] as well as the Shaker potassium channel expressed in live *Xenopus* oocytes.[18]

In this study, we demonstrate the application of LRET for investigating substrate–protein interactions between PglBs, which are polytopic membrane proteins, and their cognate substrates. PglBs are monomeric oligosaccharyl transferases (OTases) in the N-linked glycosylation systems of the Gram-negative bacteria for example of the *Campylobacter* genus.[19] N-linked glycosylation is a posttranslational modification that occurs in all domains of life[20] and has been shown to play an important role in bacterial pathogenicity in selected species including *Campylobacter jejuni*.[21] Specifically, we report LRET-based distance measurements between a Tb^{3+}-complexed N-terminal LBT as the sensitized luminescence donor complex and fluorescently labeled peptide and glycan substrates. From a practical perspective, LRET can be applied to detergent-solubilized membrane proteins affording sensitive measure-

Received: December 23, 2015
Published: February 26, 2016

DOI: 10.1021/jacs.5b13426
J. Am. Chem. Soc. 2016, 138, 3806–3812

ments using limited volumes of low μM protein samples on verifiably active targets using relatively simple instrumentation.

In the past decade, there has been considerable progress in defining the biochemical steps[22] in the bacterial protein glycosylation (pgl) pathway enzymes with recent exciting developments in the X-ray-based structure determination of the two most complex members of the pathway, PglK[23] and PglB.[24] PglK, the flippase, translocates the polyprenol diphosphate-linked glycans from the cytoplasmic to the periplasmic face of the inner membrane, and PglB mediates glycan transfer to selected asparagines in target proteins within the Asp/Glu-Xaa_1-Asn-Xaa_2-Ser/Thr consensus sequon, where Xaa_1 and Xaa_2 can be any amino acid except proline (Scheme 1). In

Scheme 1. PglB-Catalyzed Peptide Glycosylation

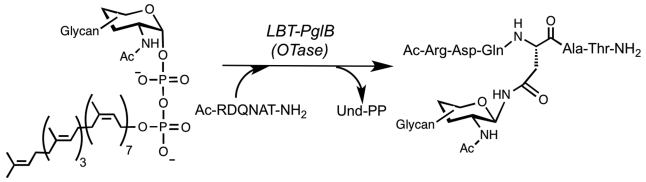

addition to the structural analysis of PglB from *Campylobacter lari* (PglB*Cl*) with a bound substrate peptide, extensive bioinformatics and biochemical studies have provided insight into optimized peptide substrate determinants,[25] the corresponding peptide binding site and potential mechanistic models for asparagine glycosylation.[26] Additionally, computational approaches have been applied to predict the structure of the undecaprenol-diphosphate-heptasaccharide (Und-PP-heptasaccharide) in complex with PglB.[27]

To validate the LRET-based approach and complement the structural data on peptide binding to the *C. lari* PglB (PglB*Cl*) we used available crystallographic data[24,28] to estimate the distances between a simulated N-terminal LBT and regions of the PglB enzyme. Then LRET was applied to complexes of the *C. jejuni* PglB (PglB*Cj*) with either peptide or glycan substrates. Distances measured by LRET in solution provide experimental evidence supporting the location and orientation of the substrate peptide (SP, Figure 1) binding to PglB*Cl* indicated in the crystal structure and show that the LRET measurements are biologically relevant. It is shown that the measured binding and orientation modes are equivalent for both PglB*Cl* and PglB*Cj*. Moreover, we have delineated the proximity of the substrates, SP and UndPP-trisaccharide, to each other when bound to PglB. We show that LRET can be applied to study the interactions of membrane enzymes with their cognate substrates, which complements the data obtained from X-ray crystallography and other biophysical and computational approaches, thereby providing a more comprehensive picture of membrane proteins in solution.

RESULTS AND DISCUSSION

Experimental Rationale. The strategy devised includes expression of PglB with a genetically encoded lanthanide-binding tag (LBT). LBTs are short peptide sequences comprising 15−20 encoded amino acids that bind lanthanide ions, such as terbium (Tb^{3+}), with high affinity and which, by virtue of a strategically placed tryptophan residue, sensitize Tb^{3+} forming a luminescent complex. These genetically encoded luminescent tags are small and the corresponding Tb^{3+} complexes have long (μs-msec) luminescence lifetimes,

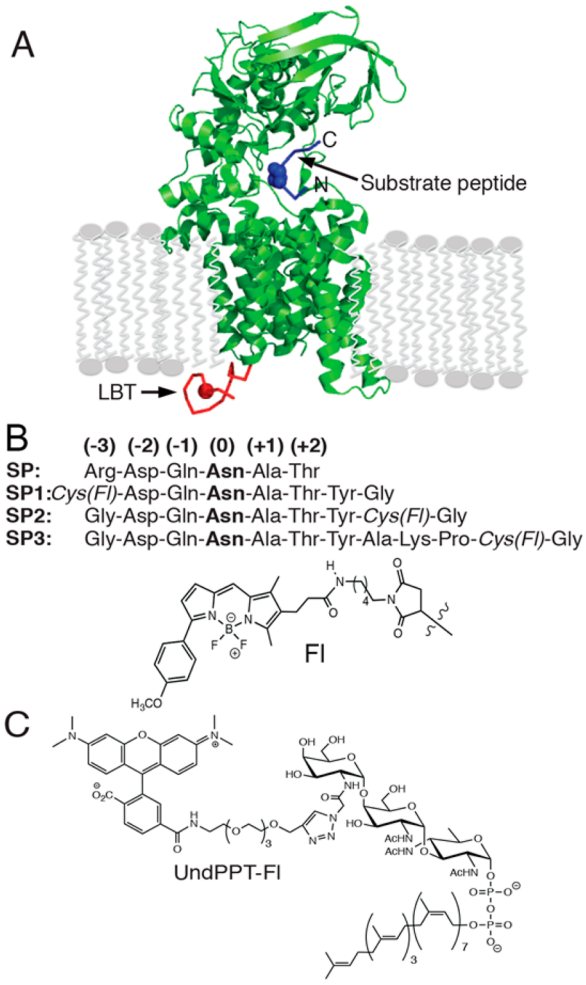

Figure 1. (A) LBT-PglB*Cl*-Δ1−12. Composite image of PglB (green) with bound substrate peptide (SP, blue), and N-terminal LBT (red) prepared using PyMol. PDB sources: 3RCE and 1TJB. The N- and C-termini of the SP are N-acetyl and C-primary amide capped respectively, and the glycosylation site (Asn) is shown in filled spheres. (B) Substrate peptides in this study with the glycosylation site (Asn) highlighted in bold. Peptides with Cys(Fl) (italic) were prepared by labeling using Bodipy-TM maleimide (Invitrogen) for LRET experiments. (C) Structure of UndPP-trisaccharide-Fl, which is the product from the Cu-catalyzed click reaction of Und-PP-diNAcBac-GalNAc-GalNAz with the acetylene-545 fluorophore reagent (Click Chemistry Tools).

which makes them ideal for LRET. There are substantial advantages of LRET over FRET.[12] The main advantage is the relatively long luminescence lifetime of a lanthanide, which allows the emission signal to be collected after a short time delay, which enables elimination of any background luminescence resulting from direct excitation of the acceptor fluorophore. Furthermore, unlike the polarized emission from fluorogenic molecules, emission from lanthanide ions is radial, resulting in a reduced error in the determination of R_0. A technical advantage with the application of LBTs to LRET is the insensitivity to incomplete probe labeling; the LBT is genetically encoded so chemical modification steps are completely avoided. All of these factors become particularly important when working with challenging membrane proteins in the presence of micelles or lipids.

Initial distance measurements between the selected LBT (MKLIFIDTNNDGWIEGDELL)[29] linked to the full length

DOI: 10.1021/jacs.5b13426
J. Am. Chem. Soc. 2016, 138, 3806−3812

PglB*Cl* (residues 1−712) and fluorescently labeled substrate peptides resulted in measured distances inconsistent with the experimental structural model of PglB*Cl*. A possible source of this disparity was the extended native *N*-terminal sequence (PglB*Cl* residues 1−12) between the LBT and the first transmembrane helix (TM1, residues 13−38). In particular, we were concerned that this linker provided flexibility in the LBT positioning with respect to PglB, possibly bringing the donor closer to the acceptor. To minimize the flexibility of the linker and position the LBT in a fixed orientation relative to TM1 of PglB, the amino acids between the LBT and the beginning of the TM1 were deleted as described in the Methods (SI). Ultimately, the new construct (LBT-PglB*Cl*-Δ1−12) with the reduced linker and more rigidly positioned LBT was analyzed for enzymatic activity, peptide substrate binding, and Tb^{3+} binding, to confirm the enzyme and the LBT function, and was used for the presented distance measurements.

Activity of LBT-PglB Construct. The attachment of the LBT to the N-terminus of PglB (Figure 1A) enables intermolecular LRET measurements between the LBT-Tb^{3+} complex and the fluorescently labeled peptides or UndPP-glycan substrates (Figure 1B and C). The LBT was encoded at the N-terminus of the PglB gene from either *C. jejuni* (for the LBT-PglB*Cj* construct) or *C. lari* (for the LBT-PglB*Cl* construct) in a vector with a C-terminal His_{10} tag (pBAD) for purification. Specifically, LBT-PglB*Cl*-Δ1−12 and LBT-PglB*Cj*-Δ1−11 were designed with N-terminal deletions on PglB to minimize the LBT → PglB linking region. The activity of both of the LBT-PglB constructs was verified with a well established radioactivity-based assay.[25] LBT-PglB*Cl*-Δ1−12 transfers glycan from UndPP-linked donor to the SP acceptor, which has a K_M similar to that with PglB*Cj* (K_M = 3.8 μM vs K_M = 0.8 μM, respectively) (Table 1). This suggests that, even with only 56% sequence identity between PglB*Cl* and PglB*Cj*, the OTases show similar peptide binding properties consistent with previous observations. Importantly, incorporation of the LBT and the N-terminal truncation of PglB do not adversely affect activity.

Table 1. Substrate Peptides K_M and K_D for PglB from *C. jejuni* and *C. lari*

	K_M (μM)[a]		
	SP	SP1	SP2
PglBCj	0.8 ± 0.11[b]	nd	nd
LBT-PglBCj		0.49 ± 0.18	0.77 ± 0.22
LBT-PglBCl	3.8 ± 1.2		
	K_D (μM)[c]		
	SP1	SP2	SP3
LBT-PglBCj	0.52 ± 0.08	0.57 ± 0.08	0.65 ± 0.05
LBT-PglBCl	1.86 ± 0.69	1.74 ± 0.94	0.87 ± 0.17

[a] K_M for a substrate peptide and PglB was determined from a best fit of the initial glycosylation rate over different peptide concentrations from the activity assay over 0.05−100 μM SP concentration and at a fixed glycan substrate concentration of 0.56 μM. [b] Value obtained from reference 25. [c] The K_D for binding of the fluorescently labeled peptides to PglB was determined from a best fit of the LRET data at different peptide concentrations represented in Figure 3. Experiments were carried out in triplicate.

Assessment of Tb^{3+} Binding to LBT. To ensure that the N-terminal LBT of PglB maintains low μM affinity binding for Tb^{3+}, each LBT-PglB construct was titrated with Tb^{3+} and sensitized luminescence was observed at 490, 544, 585, and 620 nm with the most intense band at 544 nm, which was plotted against [Tb^{3+}] to determine the K_D (Figure 2). Both constructs showed very good Tb^{3+} affinity with estimated Tb^{3+} K_Ds for PglB*Cl*-Δ1−12 = 1.8 μM and for PglB*Cj*-Δ1−11 = 2.3 μM; when each LBT-PglB construct was titrated with Tb^{3+}, the enzyme saturated at one molar equivalent of Tb^{3+} relative to the LBT-PglB (Figure 2). The selectivity and μM LBT-Tb^{3+} affinity together with the unique luminescence signal of the complex makes it an excellent LRET donor for spectroscopy with μM protein/substrate concentrations.

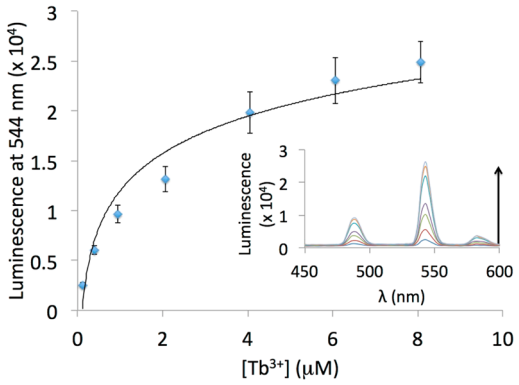

Figure 2. Binding isotherm of Tb^{3+} to 5 μM LBT-PglB*Cl*-Δ1−12. Each point represents the average of four separate experiments monitoring luminescence at 544 nm. Luminescence spectra of LBT-PglB*Cl*-Δ1−12 with Tb^{3+} at concentrations ranging from 0.11 to 8.06 μM are shown in the inset.

Evaluation of Fluorescently Labeled SP Binding to LBT-PglB Variants. The substantial overlap between the LBT-Tb^{3+} emission and the Bodipy(TMR) absorption spectrum provides the basis for LRET measurements to assess the interactions between substrates and the LBT-PglB variants. This donor−acceptor pair has also been used successfully in previous LRET experiments and has an R_0 = 50.8 Å,[30] which is in a suitable range for the targeted distance measurements. Based on the sequence of a well-characterized peptide substrate for PglB,[25] we designed peptides containing unique cysteines for fluorophore labeling (Figure 1B). In the first peptide (SP1), a cysteine was incorporated at the N-terminus, three residues from the asparagine; in the second peptide (SP2), a cysteine was positioned four residues C-terminal to the glycosylation site. The synthetic peptides, all featuring the glycosylation sequon and a cysteine residue at different positions (Figure 1B), were labeled using Bodipy-TMR maleimide and purified by HPLC. The final products were confirmed by MS (Table S2). To ensure that addition of the fluorophore did not interfere with enzyme activity, the glycosylation of labeled peptides was analyzed. The efficiency of glycan transfer to the labeled and unlabeled peptides by LBT-PglB variants was comparable. For example, the LBT-PglB*Cj* showed a K_M = 0.8 μM for unlabeled peptide, and LBT-PglB*Cj*-Δ1−11 showed a K_M = 0.49 μM and K_M = 0.77 μM for SP1 and SP2 (Table 1). This confirms that the fluorophore on the peptides and the LBT at the N-terminus of PglB do not significantly impact the interactions of the SPs with the LBT-PglB constructs or the glycan transfer reactions. The tolerance of the luminescent and fluorescent species for the assay components, namely 0.1% dodecyl maltoside, 5 mM MgCl and 10% glycerol, and the

DOI: 10.1021/jacs.5b13426
J. Am. Chem. Soc. 2016, 138, 3806−3812

unperturbed enzymatic activity supports the application of LRET to this challenging polytopic membrane enzyme.

LRET Measurements between Fluorescent SPs and LBT-PglB. LRET measurements were conducted by tryptophan excitation at 280 nm, which sensitizes luminescence of the Tb^{3+}-LBT chelate; the most intense emission band at 545 nm overlaps with the Bodipy(TMR) fluorophore excitation wavelength. In the experiments, introduction of a 50 μs time delay after excitation ensures suppression of emission signals from short-lifetime species, effectively reducing background emission and enhancing sensitivity.[12] When combined together, a reduction in the LBT-PglB luminescence and an enhancement in the SP-Bodipy(TMR)s (SP-Fls) fluorescence are consistent with LRET between the donor and acceptor (Figure 3 inset).

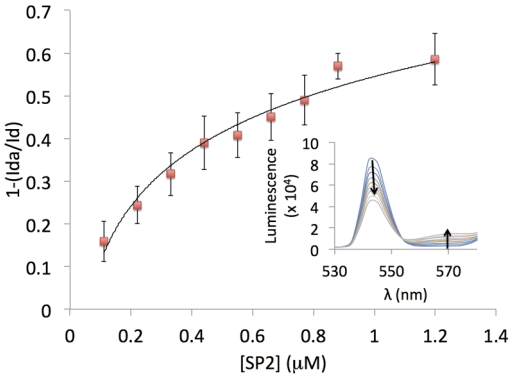

Figure 3. Binding isotherm obtained from LRET experiments of the Tb^{3+}-LBT-PglB*Cj*-Δ1−11 complex with a substrate peptide (SP2) labeled with Bodipy-TMR. Id is the luminescence intensity of the donor alone, and Ida is the luminescence intensity in the presence of a donor and acceptor at 544 nm. The decrease in the luminescence of Tb^{3+}-LBT-PglB*Cj*-Δ1−11 and the increase in the fluorescence of SP2 correlated with the increase in [SP2] from 0.028 to 1.32 μM is shown in the inset.

This was observed in a manner that was dependent on the peptide concentration. The equilibrium binding affinity of the Bodipy-labeled substrate peptide for LBT-PglB was determined based on the SP-Fl-dependent LBT luminescence quenching due to LRET (Figure 3). We observed that LRET was dependent on the concentration of SP and saturable, for example with a K_D = 0.52 ± 0.08 μM for SP1 (which is comparable to K_M = 0.49 ± 0.18 μM obtained from the activity assay for SP1; Table 1). In addition to the aforementioned activity results, these experiments further demonstrate that the fluorescently labeled substrate peptides bind specifically to both LBT-PglB*Cj*-Δ1−11 and LBT-PglB*Cl*-Δ1−12 (Table 1). Verification of specific binding between LBT-PglB and fluorescently labeled peptides sets the stage for distance measurements between these two partners using LRET.

Lifetime Decay Measurements of LBT-PglB Variants in Presence and Absence of Substrate Peptides. The Bodipy(TMR) was conjugated with the SP at different positions to derive information on binding to the LBT-PglBs using luminescence lifetime decay. To acquire a maximum luminescence signal and avoid nonspecific LRET due to nonspecific peptide binding or collisional quenching, the concentrations of the peptide used for distance measurements ranged between 40 and 80% occupancy of the PglB-substrate peptide-binding site. From the saturation binding shown in Figure 3, it is clear that these concentrations range between 0.22 μM and 0.66 μM SP. For the *C. lari* LBT-PglB-Δ1−12, in the absence of the fluorescent peptide, the LBT-Tb^{3+} luminescence lifetime is τ = 2.3 ms; in comparison, τ = 1.17 ms in the presence of SP2 (Figure 4). Addition of the acceptor

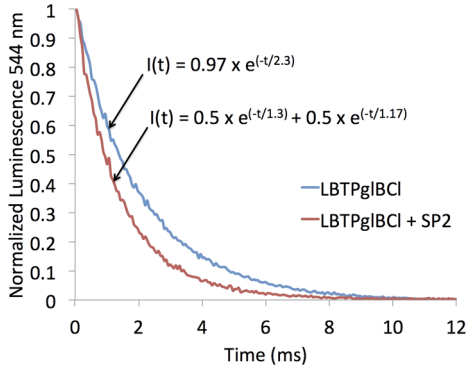

Figure 4. Lifetime measurements of 2 μM Tb^{3+}-LBT-PglB*Cl*-Δ1−12 with and without 0.66 μM SP2. The sample was excited at 280 nm with a 50 μs gate, and the luminescence decay was recorded in 60 μs increments. The lifetime decay data were fit to mono- or biexponential equations, $I(t) = I(0) \times e^{-t/\tau_D}$ or $I(t) = I(0)_1 \times e^{-t/\tau_D} + I(0)_2 \times e^{-t/\tau_{DA}}$, respectively.

leads to a more rapid decay rate, indicating LRET. There was no change in the lifetime decay of the donor upon addition of the unlabeled SP, indicating that the peptide alone does not influence the donor lifetime.

Distance Measurements between SP and LBT-PglB. The structural basis of peptide recognition by the *C. lari* PglB has been determined by X-ray crystallography. The capacity to measure distances[24] with Å-resolution using LRET[12,13] allows an independent analysis of peptide binding to PglB in solution. To estimate the relevant distances, PyMol was used to model the structure of the LBT (PDB: 1TJB) onto the crystal structure of PglB from *C. lari* (PDB: 3RCE),[24] taking into consideration the N-terminal truncation. Using this model as a guide, the distances from the center of the chelated Tb^{3+} donor to the approximate fluorophore location when attached to the acceptor peptides were determined (Figure 1A and Table 2). Specifically, to simplify the modeling of distance measurements, we substituted a tryptophan at the cysteine site and then measured distances from the Tb^{3+} center in the LBT to the C-5

Table 2. Distance Measurements between LBT-PglB and Substrates

	measured distance (Å)[b]		modeled distance (Å)[c]
substrate[a]	*C. lari*	*C. jejuni*	*C. lari*
SP1	51.6 ± 2.0	52.4 ± 3.3	55
SP2	54.1 ± 0.8	54.8 ± 3.7	59
SP3	51.4 ± 1.5	51.4 ± 2.2	ND[d]
UndPPT-Fl	58.7 ± 3.5	59.5 ± 3.7	

[a]Substrate peptides (SP) labeled with Bodipy-TM maleimide and Und-PP-diNAcBac-GalNAc-GalNAz substrate labeled with Acetylene-Fluor 545 (UndPPT-Fl) are shown in Figure 1B and C. [b]Distance measurements ware calculated from LBT-Tb^{3+} lifetime decay data as shown in Figure 4 and 6. Data were averaged over a range of substrate concentrations and experiments were repeated in triplicate. Average distances with STDEV indicated. [c]The distance was measured between the modeled N-terminal LBT tag and the substrate peptide as illustrated in Figure 1A. [d]Information not available from 3RCE.

DOI: 10.1021/jacs.5b13426
J. Am. Chem. Soc. 2016, 138, 3806−3812

of the indole ring for SP1 and SP2. Lifetime decays of LBT-Tb^{3+} in the presence of fluorescently labeled SPs together with Förster theory were applied to experimentally determine the distances between the LBT and three distinct sites on the SP. The average distances were calculated as described in the Methods (SI). The distances, measured by LRET, from the Tb^{3+} to the Bodipy on the SP1 and SP2 are R = 51.6 Å and R = 54.1 Å for the *C. lari* enzyme, respectively. Due to the existence of a flexible linker between the fluorophore and the point of attachment to the SP (Figure 1B), the exact placement of the fluorophore with respect to the peptide is uncertain. If the linker is flexible, we anticipate obtaining average distance measurements using LRET. Nevertheless, consistent with the modeled distances on the crystal structure, we found that the probe on the SP1 is closer to the LBT than the probe on SP2. To further evaluate the position of the peptide in the binding site, we elongated the C-terminus of the SP used in the crystal structure by extending the length by adding four naturally occurring amino acids taken from the sequence of the glycoprotein PEB3,[31] placing the cysteine seven residues away from the glycosylation site (+7) (SP3 in Figure 1B). Interestingly, the experimentally determined distance from the LBT to this residue was 51.4 Å, bringing the (+7) residue closer to the N-terminus of the PglB than the (+4) residue. This suggests that the peptide forms a turn in the binding site, positioning the (−3) and (+4) amino acids of the SP in close proximity.

Comparison of the distances calculated between the Tb^{3+}-bound LBT-PglB*Cl*-Δ1−12 and SP1 and SP2 with measurements based on the reported structure provide excellent validation for the LRET approach with this complex polytopic membrane enzyme. In light of these results we then applied parallel methods and reagents to the *C. jejuni* enzyme construct, LBT-PglB*Cj*-Δ1−12. The *C. jejuni* and *C. lari* PglBs show 56% identity. The *C. jejuni* enzyme is of interest because it was the first characterized bacterial OTase and it is the homologue that has been the subject of the majority of the biochemical studies, although it has proven intractable to structure determination. The distances measured with LBT-PglB*Cl*-Δ1−12 were comparable to those for LBT-PglB*Cj*-Δ1−11 (Table 2), suggesting that the tertiary fold of both protein structures is similar. This information is of considerable value as it suggests that the known structure of the *C. lari* PglB is a useful guide for studies on the *C. jejuni* homologue.

LRET Measurements between UndPPT-Fl and LBT-PglB. Azido sugar substrates are well tolerated by several of the *C. jejuni* biosynthetic Pgl pathway enzymes, enabling the chemoenzymatic synthesis of azide modified glycan substrates that are amenable to click chemistry for conjugating the fluorophore.[32] In the context of the current study, it was also shown that PglB*Cj* tolerates Und-PP-diNAcBac-GalNAc-GalNAz conjugated to acetylene-545 fluorophore (UndPPT-Fl) as a glycosyl donor substrate. The absorption of the 545 fluorophore overlaps with the main Tb^{3+}-LBT emission band (λ_{max} at 544 nm), making it a suitable acceptor for LRET and the R_0 for the LBT-Tb^{3+} donor and the 545 fluorophore acceptor was calculated (as described in the Methods (SI)) to be 58.2 Å. Prior to the distance calculations, the binding constant for the glycan substrate was determined using LRET. The values obtained were K_D = 0.33 ± 0.07 μM for LBT-PglB*Cl*-Δ1−12 and K_D = 0.1 ± 0.03 μM for LBT-PglB*Cj*-Δ1−11. A decrease in the luminescence of LBT-Tb^{3+} and a concomitant increase in the fluorescence of 545 fluorophore with Und-PPT-Fl titration (Figure 5 inset) were observed, with saturation of the energy transfer (Figure 5).

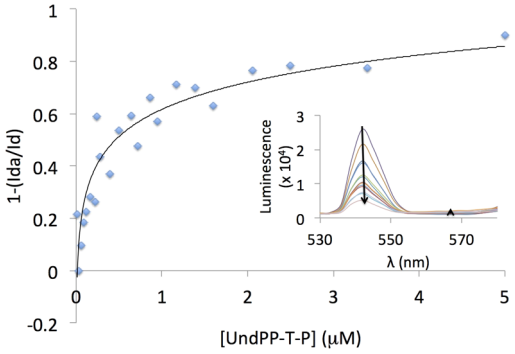

Figure 5. Binding isotherm obtained from LRET experiments of Tb^{3+}-LBT-PglB*Cl*-Δ1−12 complex with Und-PP-diNAcBac-GalNAc-GalNAz conjugated with acetylene-545 fluorophore (UndPPT-Fl). Id is the luminescence intensity of the donor alone and Ida is the luminescence intensity in presence of the donor and acceptor at 544 nm. Spectra reflecting LRET between the Tb^{3+}-LBT-PglB*Cl*-Δ1−12 complex and [UndPPT-Fl] from 0.014 to 5 μM are shown in the inset.

Distance Measurements between UndPPT-Fl and LBT-PglB. To determine the distance between the N-terminal Tb^{3+}-LBT complex and UndPPT-Fl, lifetime decay experiments were again performed. Consistent with LRET, a decrease in the lifetime decay was observed in the presence of the substrate (Figure 6). These data were used to calculate the distances

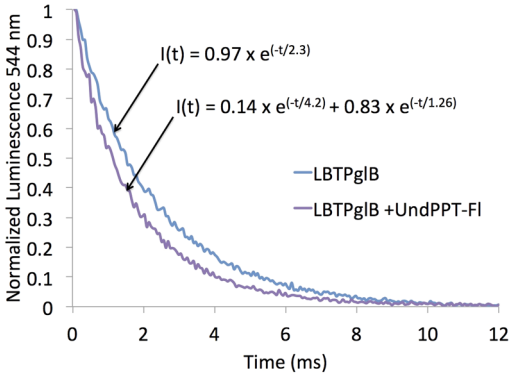

Figure 6. Lifetime measurements of 2 μM Tb^{3+}-LBT-PglB with and without 0.66 μM Und-PP-diNAcBac-GalNAc-GalNAz conjugated with acetylene-545 fluorophore (UndPPT-Fl). The sample was excited at 280 nm with 50 μs gate, and the luminescence decay was recorded at 60 μs increments. The lifetime decay data were fit to mono- or biexponential equations, $I(t) = I(0) \times e^{-t/\tau_D}$ or $I(t) = I(0)_1 \times e^{-t/\tau_D} + I(0)_2 \times e^{-t/\tau_{DA}}$, respectively.

between the donor and the acceptor as described for the SP interactions. The studies indicate that the fluorophore on the trisaccharide is positioned 58.7 ± 3.5 Å from Tb^{3+}-LBT on LBT-PglB*Cl*-Δ1−12 and 59.5 ± 3.7 Å from Tb^{3+}-LBT on LBT-PglB*Cj*-Δ1−11 (Table 2), supporting these OTases also have similar glycan substrate binding interactions and overall structures. In this case, it is not realistic to predict absolute distances from a structural model, because the distance between the triazole, introduced by click chemistry, and the fluorophore is extended due to the flexible PEG linker in the commercially derived acetylene reagent (Figure 1C). However, it is noteworthy that the current measurements are consistent

DOI: 10.1021/jacs.5b13426
J. Am. Chem. Soc. 2016, 138, 3806−3812

with a recently proposed computational model of the interaction.[27] In the future, it will be necessary to make additional complementary measurements from LBTs at other sites in PglB, for example positioned in the cytoplasmic loops.[33] LRET studies on these additional constructs will then serve to localize the glycan binding site, in contrast to the current studies, which only provide two points of reference, the Tb^{3+} in the LBT and the fluorophore, and while the LBT position is known relative to the frame of the protein, the fluorophore could be anywhere on the sphere that is predicted by the measured distance.

CONCLUSION

We have applied a molecular ruler based on LRET to measure the distances between a genetically encoded luminescence donor, LBT-Tb^{3+}, attached to the N-terminus of an integral polytopic membrane protein, and fluorescent acceptors conjugated to the cognate substrates for two related oligosaccharyl transferases (PglBs). The strategy was validated by first deriving distance information consistent with measured parameters from the crystal structure of a peptide substrate bound to the *C. lari* PglB[24] and then performing comparative studies on the interactions of the cognate peptide and glycan substrates with both the *C. lari* and *C. jejuni* PglBs. This methodology is compatible with limited sample concentrations (2−5 μM) and volumes (100−200 μL) as well a number of buffer additives that are important for the stabilization of membrane proteins including selected cations, detergent and glycerol. The studies presented herein are also readily adaptable for investigating potential conformational changes of PglB involved in substrate binding and catalysis by employing the N-terminal Tb^{3+}-LBT as a luminescence donor together with cysteine labeling to install Bodipy(TMR) as an acceptor onto discrete sites in the PglB, which would provide intramolecular distance measurements and, therefore, shed light on the intrinsic conformational changes of PglB due to substrate binding. In addition, application of LBTs at alternate defined sites in loops and at the protein termini should allow more definition concerning the location of fluorescently labeled substrates on the enzyme. Furthermore, there will also be opportunities for using LRET as a readout for screening for competitive binders to the peptide and glycan binding sites as reported previously in an RNA polymerase HTS screen.[34]

We are confident that these studies described herein will promote the more widespread application of LRET, enabled by encoding LBTs at the N- or C-termini and into defined loop regions,[33] to other polytopic membrane proteins of broad interest to the chemical and biological communities.

ASSOCIATED CONTENT

Supporting Information

The Supporting Information is available free of charge on the ACS Publications website at DOI: 10.1021/jacs.5b13426.

Supporting experimental methods include protein expression and purification approaches, protocols for synthetic substrate preparation and detail of luminescence measurements. Supporting tables include a listing of primers and mass spectrometry data. (PDF)

AUTHOR INFORMATION

Corresponding Author

*imper@mit.edu

Present Address

[§]Centers for Disease Control and Prevention, Atlanta, Georgia, United States.

Notes

The authors declare no competing financial interest.

ACKNOWLEDGMENTS

This research was supported by NIH GM-039334 (B.I. and M.M.), NSF Grant MCB 0744415 and the NIH Pre-Doctoral Training Grant T32GM007287 (M.B.J.). We thank Drs. Garrett Whitworth and Vinita Lukose for the synthesis and labeling of UndPP-trisaccharide.

REFERENCES

(1) Krogh, A.; Larsson, B.; von Heijne, G.; Sonnhammer, E. L. *J. Mol. Biol.* **2001**, *305*, 567.
(2) White, S. H. *Nature* **2009**, *459*, 344.
(3) Moraes, I.; Evans, G.; Sanchez-Weatherby, J.; Newstead, S.; Stewart, P. D. *Biochim. Biophys. Acta, Biomembr.* **2014**, *1838*, 78.
(4) Overington, J. P.; Al-Lazikani, B.; Hopkins, A. L. *Nat. Rev. Drug Discovery* **2006**, *5*, 993.
(5) Gubellini, F.; Verdon, G.; Karpowich, N. K.; Luff, J. D.; Boel, G.; Gauthier, N.; Handelman, S. K.; Ades, S. E.; Hunt, J. F. *Mol. Cell. Proteomics* **2011**, *10*, M111.007930.
(6) Carpenter, E. P.; Beis, K.; Cameron, A. D.; Iwata, S. *Curr. Opin. Struct. Biol.* **2008**, *18*, 581.
(7) Stansfeld, P. J.; Goose, J. E.; Caffrey, M.; Carpenter, E. P.; Parker, J. L.; Newstead, S.; Sansom, M. S. *Structure* **2015**, *23*, 1350.
(8) Liao, M.; Cao, E.; Julius, D.; Cheng, Y. *Curr. Opin. Struct. Biol.* **2014**, *27*, 1.
(9) Nannenga, B. L.; Shi, D.; Leslie, A. G.; Gonen, T. *Nat. Methods* **2014**, *11*, 927.
(10) Baker, L. A.; Baldus, M. *Curr. Opin. Struct. Biol.* **2014**, *27*, 48.
(11) Selvin, P. R.; Hearst, J. E. *Proc. Natl. Acad. Sci. U. S. A.* **1994**, *91*, 10024.
(12) Selvin, P. R. *Annu. Rev. Biophys. Biomol. Struct.* **2002**, *31*, 275.
(13) Zherdeva, V. V.; Savitsky, A. P. *Biochemistry (Moscow)* **2012**, *77*, 1553.
(14) Franz, K. J.; Nitz, M.; Imperiali, B. *ChemBioChem* **2003**, *4*, 265.
(15) Posson, D. J.; Ge, P.; Miller, C.; Bezanilla, F.; Selvin, P. R. *Nature* **2005**, *436*, 848.
(16) Posson, D. J.; Selvin, P. R. *Neuron* **2008**, *59*, 98.
(17) Vazquez-Ibar, J. L.; Weinglass, A. B.; Kaback, H. R. *Proc. Natl. Acad. Sci. U. S. A.* **2002**, *99*, 3487.
(18) Sandtner, W.; Bezanilla, F.; Correa, A. M. *Biophys. J.* **2007**, *93*, L45.
(19) Szymanski, C. M.; Yao, R.; Ewing, C. P.; Trust, T. J.; Guerry, P. *Mol. Microbiol.* **1999**, *32*, 1022.
(20) Larkin, A.; Imperiali, B. *Biochemistry* **2011**, *50*, 4411.
(21) Szymanski, C. M.; Wren, B. W. *Nat. Rev. Microbiol.* **2005**, *3*, 225.
(22) Glover, K. J.; Weerapana, E.; Imperiali, B. *Proc. Natl. Acad. Sci. U. S. A.* **2005**, *102*, 14255.
(23) Perez, C.; Gerber, S.; Boilevin, J.; Bucher, M.; Darbre, T.; Aebi, M.; Reymond, J. L.; Locher, K. P. *Nature* **2015**, *524*, 433.
(24) Lizak, C.; Gerber, S.; Numao, S.; Aebi, M.; Locher, K. P. *Nature* **2011**, *474*, 350.
(25) Chen, M. M.; Glover, K. J.; Imperiali, B. *Biochemistry* **2007**, *46*, 5579.
(26) Gerber, S.; Lizak, C.; Michaud, G.; Bucher, M.; Darbre, T.; Aebi, M.; Reymond, J. L.; Locher, K. P. *J. Biol. Chem.* **2013**, *288*, 8849.
(27) Kern, N. R.; Lee, H. S.; Wu, E. L.; Park, S.; Vanommeslaeghe, K.; MacKerell, A. D., Jr.; Klauda, J. B.; Jo, S.; Im, W. *Biophys. J.* **2014**, *107*, 1885.
(28) Nitz, M.; Sherawat, M.; Franz, K. J.; Peisach, E.; Allen, K. N.; Imperiali, B. *Angew. Chem., Int. Ed.* **2004**, *43*, 3682.
(29) Nitz, M.; Franz, K. J.; Maglathlin, R. L.; Imperiali, B. *ChemBioChem* **2003**, *4*, 272.

DOI: 10.1021/jacs.5b13426
J. Am. Chem. Soc. 2016, 138, 3806−3812

(30) Sculimbrene, B. R.; Imperiali, B. *J. Am. Chem. Soc.* **2006**, *128*, 7346.
(31) Rangarajan, E. S.; Bhatia, S.; Watson, D. C.; Munger, C.; Cygler, M.; Matte, A.; Young, N. M. *Protein Sci.* **2007**, *16*, 990.
(32) Lukose, V.; Whitworth, G.; Guan, Z.; Imperiali, B. *J. Am. Chem. Soc.* **2015**, *137*, 12446.
(33) Barthelmes, K.; Reynolds, A. M.; Peisach, E.; Jonker, H. R.; DeNunzio, N. J.; Allen, K. N.; Imperiali, B.; Schwalbe, H. *J. Am. Chem. Soc.* **2011**, *133*, 808.
(34) Glaser, B. T.; Bergendahl, V.; Thompson, N. E.; Olson, B.; Burgess, R. R. *Assay Drug Dev. Technol.* **2007**, *5*, 759.

DOI: 10.1021/jacs.5b13426
J. Am. Chem. Soc. 2016, 138, 3806−3812